Hydrothermal Preparation of Apatite-Type Phases La$_{9.33}$Si$_6$O$_{26}$ and La$_9$M$_1$Si$_6$O$_{26.5}$ (M = Ca, Sr, Ba)

Atiek Rostika Noviyanti[1,2], Bambang Prijamboedi[1], I Nyoman Marsih[1] & Ismunandar[1,*]

[1]Inorganic and Physical Chemistry Division, Faculty of Mathematics and Natural Sciences, Institut Teknologi Bandung, Jalan Ganesha 10 Bandung, Jawa Barat 40132, Indonesia
[2]Present address: Department of Chemistry, Padjadjaran University Jl. Raya Bandung-Sumedang Km. 21 Bandung, Jawa Barat 45363, Indonesia
*E-mail: ismu@chem.itb.ac.id

Abstract. Apatite-type lanthanum silicates show a great potential to be used as an electrolyte for intermediate- to low-temperature (600-700 °C) solid oxide fuel cells (ITSOFC). However, so far these materials need to be prepared using a very high-temperature method, thus there is a growing interest to prepare apatites at lower temperatures. This paper reports the synthesis of undoped La$_{9.33}$Si$_6$O$_{26}$ and doped apatites (La$_9$CaSi$_6$O$_{26.5}$, La$_9$SrSi$_6$O$_{26.5}$, and La$_9$BaSi$_6$O$_{26.5}$) from raw materials La$_2$O$_3$, Na$_2$SiO$_4$, BaCO$_3$, CaCO$_3$, and SrCO$_3$ using a hydrothermal method. The polycrystalline apatites were obtained as a white powder, after the basic solution of the reagent mixture was heated at 240 °C in an autoclave for 3 days. Le Bail refinement of the X-ray powder diffraction data showed that the compounds have a hexagonal cell (*P 6$_3$/m* space group). In this paper, the undoped La$_{9.33}$Si$_6$O$_{26}$ and La-doped apatite ionic conductivities are also presented.

1   Introduction

Oxygen ionic conductors are materials of numerous great potential applications in devices such as sensors [1], oxygen pumps [2] and fuel cells [3]. Recently, a range of rare-earth apatite materials have been proposed as alternative solid electrolyte materials, following the exciting discovery of fast oxide-ion conductivity in silicate-based systems [4]. Apatite-type lanthanum silicate oxide materials have the general formula La$_{9.33+x}$(SiO$_4$)$_6$O$_{2+3x/2}$. They consist of an isolated SiO$_4$ tetrahedral with the lanthanum cations located in two cavity sites, one with 7 coordination numbers and the other with 9 coordination numbers. The extra oxygen atoms occupy channels running through the structure that are responsible for the high oxygen ion conduction [5].

Various synthetic methods have been used to prepare apatite-type materials, such as solid state reaction, sol-gel processing and mechanical milling. High-temperature (> 1350 °C) solid state reaction is the most commonly used method [6]. There is a growing interest in preparing apatites at lower temperatures [5]. Low-temperature methods such as mechanical milling [7], sputtering [8,9], plasma spraying [10,11] and sol-gel processing [12] have been applied successfully for the synthesis of oxyapatites. Hydrothermal treatments have also been used to synthesize isostructural apatites, i.e. hydroxyapatite [13], and terbium and lanthanum silicate apatite [14].

Among the synthesis methods to prepare solid oxides, hydrothermal methods have many advantages over other fabrication techniques. They give solid oxides with high homogeneity and purity at a much lower reaction temperature [14,15]. It is also noted that the preparation of terbium and lanthanum silicate apatite prepared with a hydrothermal method still yakes a long time to complete (168 h at 230 °C). It would be of great advantage if the apatite can be prepared at a lower temperature, in a shorter time, and with high reproducibility. It is also of great importance to find a proper precursor for apatite synthesis through a hydrothermal process at low temperature. The application of a hydrothermal method to prepare doped lanthanum silicate apatites has never been done before. The modification of the apatite composition by introducing dopants is a common route to obtain an apatite with the desired characteristics. The latter is important since, in general, the search for the best electrolyte in the apatite system is carried out using a doping strategy.

This paper reports the preparation of $La_{9.33}Si_6O_{26}$ and doped lanthanum silicate apatite using hydrothermal methods from various precursors. The structure and microstructure of the obtained material were investigated by X-ray powder diffraction and scanning electron microscope (SEM) measurements. Oxide ion conductivity of the apatites was also measured and analyzed.

2   Experiment

High-purity La_2O_3 (Aldrich, 99.999%), Na_2SiO_3 (Sigma, 97%), $BaCO_3$ (Aldrich 99,98%), $CaCO_3$ (Aldrich 99,995%), and $SrCO_3$ (Aldrich 99,995%) were used to prepare apatite-type phase $La_{9.33}Si_6O_{26}$, $La_9CaSi_6O_{26,5}$, $La_9SrSi_6O_{26,5}$, and $La_9BaSi_6O_{26,5}$. A NaOH 3 M solution was used in the preparation of these apatites as mineralizer. The La_2O_3 was pre-calcined at 1100 °C for 12 h in order to achieve decarbonation. In a typical experiment for preparing $La_{9.33}Si_6O_{26}$, a stoichiometric weight of La_2O_3 (3.2330 g) and Na_2SiO_3 (1.5581 g) were thoroughly mixed and added to the NaOH solution, after which the mixtures were transferred into a stainless steel autoclave (302 AC Bombs Parts 105 mL)

until 60 % volume of the autoclave was occupied. After being heated at 240 °C for 3 days, the precipitate was collected by filtration and washed with demineralized water. The resulting powder was dried at 120°C. The powder X-ray diffraction (XRD) of the apatite was measured with a PW 3373 PANalytical using Cu-K$_\alpha$ radiation. The elemental analysis was carried out by XRF measurement. Ionic conductivity was measured using an LCR meter (Agilent E4980A) at 175-500 °C and a frequency range of 20 Hz – 2 MHz on the pellet sample that was obtained by applying 6000 kg cm^{-2} pressure, followed by sintering at 1100 °C for 12 h and at 1600°C for 3 h.

3   Results and Discussion

The XRD patterns of the La$_{9.33}$Si$_6$O$_{26}$ powder, obtained through a hydrothermal process followed by heating at various temperatures, are shown in Figure 1. There was no change in the XRD diffraction pattern of the apatite powder after being dried at different temperatures, although the peaks became sharper in the diffractogram of the sample that received heat treatment at higher temperatures. The La$_{9.33}$Si$_6$O$_{26}$ phase has been identified in the powder which was dried at 120°C. This means that the La$_{9.33}$Si$_6$O$_{26}$ phase has been formed during the hydrothermal process, and calcination at higher temperature increased its crystallinity. According to the analysis of the XRD data using the Le Bail method, the synthesized La$_{9.33}$Si$_6$O$_{26}$ adopts the *P 63/m* space group.
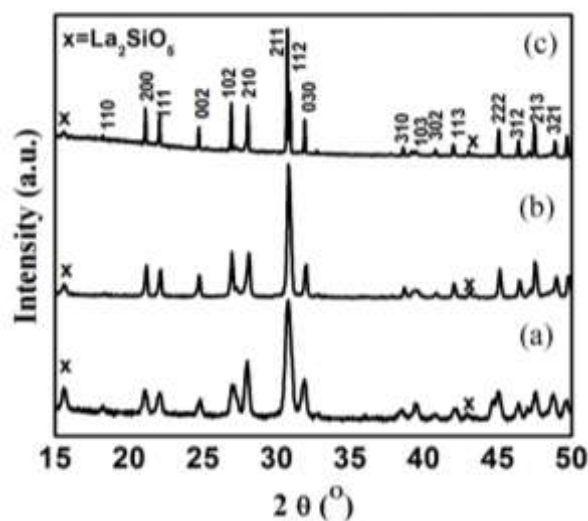

Figure 1 XRD pattern of La$_{9.33}$Si$_6$O$_{26}$ synthesized by a hydrothermal method at 240 °C for 3 days, dried and heated at (a) 120 °C for 24 h, (b) 1100 °C for 17 h and (c) 1600 °C for 3 h; hkl indicates the possible Bragg reflections of the apatite phase.
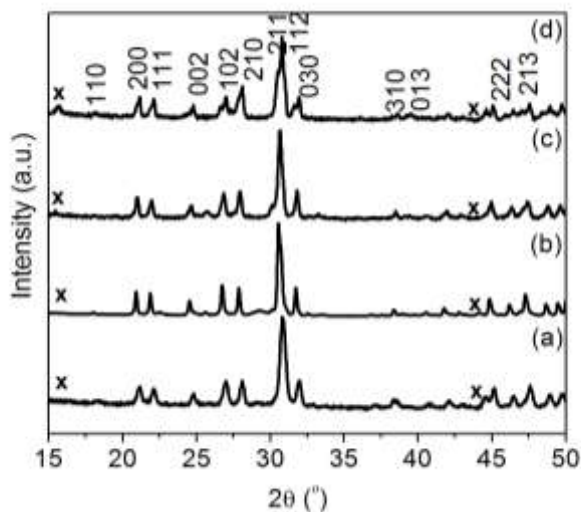
Figure 2 XRD patterns of apatites (a) $La_{9.33}Si_6O_{26}$ (b) $La_9CaSi_6O_{26.5}$ (c) $La_9SrSi_6O_{26.5}$ (d) and $La_9BaSi_6O_{26.5}$.

The lattice parameters of $La_{9.33}Si_6O_{26}$ obtained from the refinement of XRD patterns of the apatite sample after sintering at different temperatures were similar, indicating that the structure was stable. The lattice parameters of our sample after sintering at 1600°C were $a = b = 9.7308(4)$, and $c = 7.1923 (3)$ Å, and these values are in a good agreement with the reported data [16]. Elemental analysis (XRF) gave the formula of the synthesized apatite to be $La_{9.59}Si_6O_{26.39}$ approximately, which is very close to the expected formula ($La_{9.33}Si_6O_{26}$). Composition of lanthanum in the apatite was slightly higher than that expected from the starting material, however the difference is still within the measurement error range ($La_{9.59 \pm 0.162}$). XRF analysis also gave a Na composition of 1,6 ± 0,097, as a result of partial substitution at the La site; a similar observation was also reported in the literature [14]. Following the XRD and XRF analysis as described above, we concluded that the $La_{9.33}Si_6O_{26}$ apatite had been formed. In addition, the XRD patterns of the doped apatites are similar to those of $La_{9.33}Si_6O_{26}$ (Figure 2), indicating that reaction conditions of $La_{9.33}Si_6O_{26}$, have been successfully applied to prepare doped apatite. The unit cell parameters of the doped apatites are given in Table 1. The unit cell parameters, as expected, increase as Ba substitutes La, Ba^{2+} cation is larger than La^{3+} (r Ba^{2+} = 1.52 Å and r La^{3+} = 1.24 Å Coordination Number (CN) = 7). Calcium doping, on the contrary, leads to a contraction of the cell volume (r Ca^{2+} = 1.20 Å CN7). Strontium (r Sr^{2+} = 1.21 Å, CN7) doping gives an increase in the c parameter and a decrease in the a-axis parameter, and a smaller cell volume than that of the parent apatite. This result is in good agreement with the previous studies on strontium doped apatite [17].

Table 1 The unit cell parameters (hexagonal cell) for undoped and doped apatites.

Composition	$a = b$ (Å)	c (Å)	Cell volume (Å^3)
$La_9CaSi_6O_{26.5}$	9.694(1)	7.180(1)	584.358(9)
$La_9SrSi_6O_{26.5}$	9.718(1)	7.193(1)	588. 257(1)
$La_9BaSi_6O_{26.5}$	9.730(1)	7.197(1)	590.076(5)
$La_{9.33}Si_6O_{26}$	9.722(1)	7.188(1)	588.458(2)

A secondary phase was found in the apatite, which was identified as La_2SiO_5, as can be seen from its characteristic peaks around $2\theta = 15^o$ and 44°. This phase was also observed in the sample prepared by solid state reaction [16] and sol gel processing. The thermodynamical La_2SiO_5 phase is more stable than the $La_{9.33}Si_6O_{26}$ apatite below 1600 °C [16], therefore La_2SiO_5 phase is often found in the product of apatite synthesis.
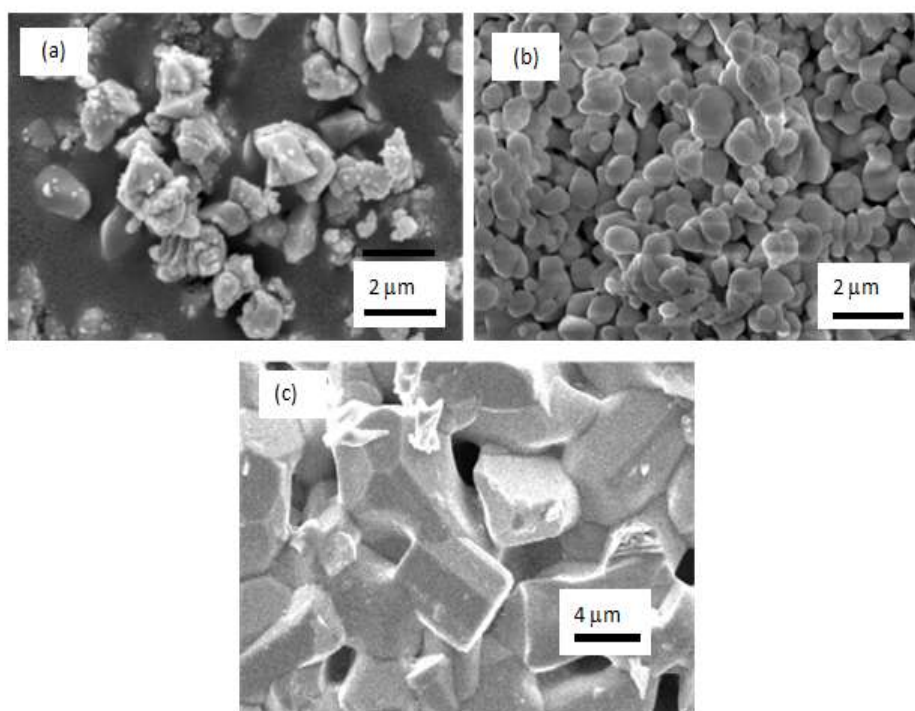
Figure 3 Micrograph of $La_{9.33}Si_6O_{26}$ phase dried at (a) 120 °C for 24 h and sintered at (b) 1100 °C for 17 h and (c) 1100 °C for 12 h then at 1600 °C for 3 h.
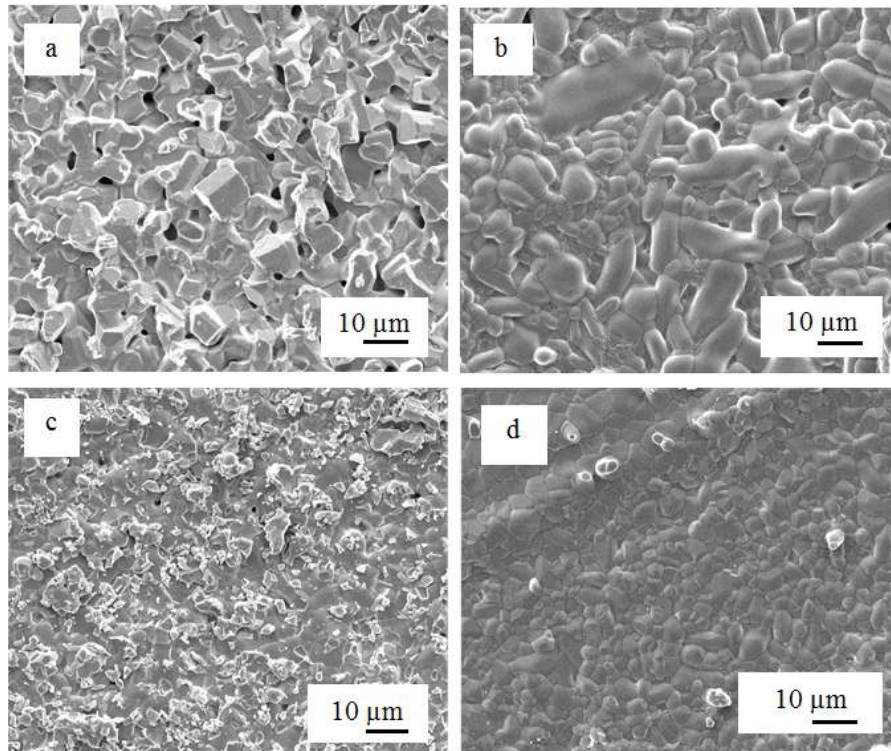
Figure 4 Micrograph of apatites (a) $La_{9.33}Si_6O_{26}$ (b) $La_9BaSi_6O_{26.5}$ (c) $La_9SrSi_6O_{26.5}$ and (d) $La_9CaSi_6O_{26.5}$ after being sintered at 1100°C for 12 h then at 1600°C for 3 h.

SEM micrographs of $La_{9.33}Si_6O_{26}$ apatite phases prepared by a hydrothermal method and sintered at different temperatures, are shown in Figure 3. As the sintering temperature was increased from 120 to 1600 °C, the grain size of $La_{9.33}Si_6O_{26}$ increased from about 1 μm (Figure 3a) to about 4 μm (Figure 3c). This is consistent with the fact that the XRD diffractogram of $La_{9.33}Si_6O_{26}$ sintered at 1600 °C has sharper peaks than that of $La_{9.33}Si_6O_{26}$ sintered at other temperatures. High temperatures (> 1600 °C) are needed to make a dense sample, while sintering at lower temperatures (1100 °C), even for a longer time (17 h), does not result in a dense apatite. It has been reported frequently that dense sintered lanthanum silicates are difficult to obtain using solid state reaction [16] and sol gel methods [12]. SEM micrographs (Figure 4) show the existence of significantly different features in the microstructure of the dense pellet depending on the composition. In Figure 4a, the undoped apatite ($La_{9.33}Si_6O_{26}$) exhibited a larger grain size and higher porosity than that of the doped apatites. Doping of apatites increases the degree of compactness of the

pellet and decreases grain size. The relative densities and average grain sizes of these apatites are reported in Table 2.

Table 2   Relative densities and grain sizes of undoped and doped apatites.

Composition	Relative Density (%)	Particle size (μm)
$La_9CaSi_6O_{26.5}$	96,4	2,5
$La_9SrSi_6O_{26.5}$	77,2	2,6
$La_9BaSi_6O_{26.5}$	84,1	3,3
$La_{9.33}Si_6O_{26}$	82,5	3,4

The Nyquist plot obtained at 300 °C for $La_{9.33}Si_6O_{26}$ apatite is presented in Figure 5. The complex impedance plots of $La_{9.33}Si_6O_{26}$ were similar to the impedance plots of $La_{9.33}Si_6O_{26}$ (at 310 °C) obtained by solid state reaction [16]. Both almost have the same shape but are different in their grain boundary response. The plot shows three semicircles: the high-frequency region corresponds to the bulk response, whereas the medium-frequency region is related to the grain boundary contribution, and the low-frequency region is due to the electrode interface contribution.
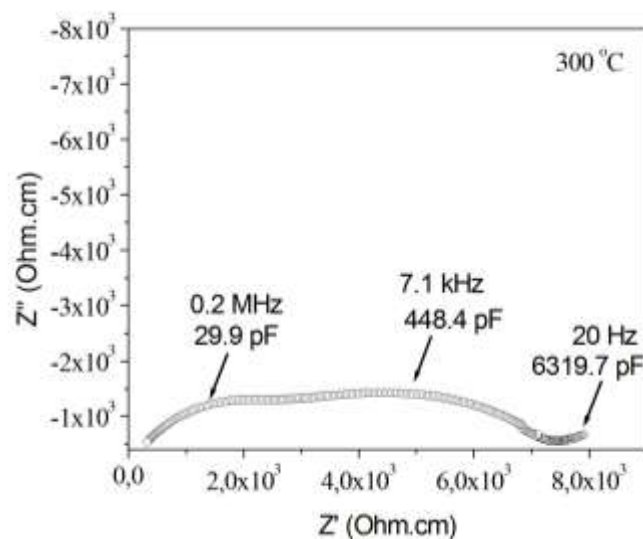

Figure 5   Complex impedance plots of $La_{9.33}Si_6O_{26}$ compound at 300°C.

An Arrhenius plot of the total ionic conductivity of $La_{9.33}Si_6O_{26}$ phase sintered at 1600°C for 3 h is shown in Figure 6. This apatite has a total conductivity of 2.9 × 10^{-4} S cm^{-1} at 500 °C; this value is comparable to the reported conductivity value of $La_{9.33}Si_6O_{26}$ synthesized by solid state reaction [16]. A different

synthesis method could give a slightly different conductivity value, as reported previously [18]. The conductivity of doped apatites increases from $La_9CaSi_6O_{26,5}$, $La_9SrSi_6O_{26,5}$, to $La_9BaSi_6O_{26,5}$ (Table 3). These results also highlight the influence of the dopant size (as dopant size increases from Ca, Sr to Ba) on the apatite; the doped apatites had lower conductivity compared to the parent compound. Similar observation results have been reported for doped apatites prepared by using a solid state technique [19]. The best conductivity at 500 °C is observed for the barium doped apatite (2.53×10^{-4} S cm^{-1} at 500 °C), followed by the strontium and calcium doped apatites.

Table 3　Conductivities and activation energies of undoped and doped apatites.

Composition	Conductivity at 500°C (S cm^{-1})	Activation energy (eV) (low temperature/high temperature slopes)
$La_9CaSi_6O_{26.5}$	1.38×10^{-4}	0.80
$La_9SrSi_6O_{26.5}$	2.07×10^{-4}	0.81
$La_9BaSi_6O_{26.5}$	2.53×10^{-4}	0.78
$La_{9.33}Si_6O_{26}$	2.95×10^{-4}	0.49/0.83

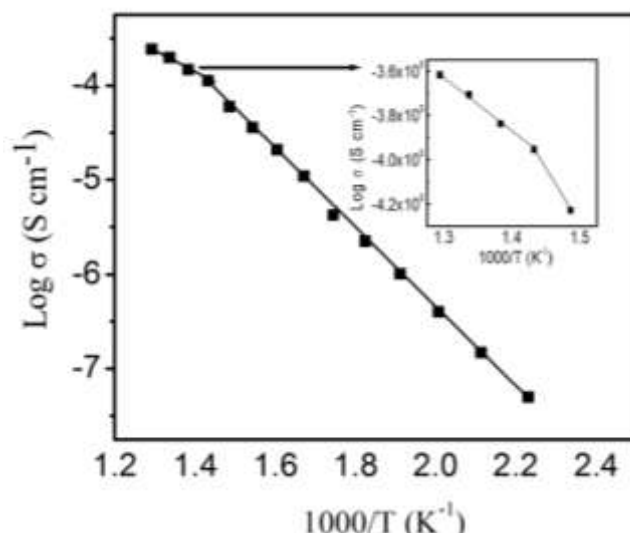**Figure 6**　Arrhenius plot of the ionic conductivity of $La_{9.33}Si_6O_{26}$ phase, sintered at 1600 °C for 3 h. The insert is a zoom of the five highest temperature plots.

The activation energy of $La_{9.33}Si_6O_{26}$, E_a significantly decreases from 0.83 eV below 425 °C to 0.49 eV above 425 °C. It has been concluded previously that in apatite oxide materials, an activation energy below 1.1 eV indicates that the ionic conduction arises from the migration of interstitial oxide ions [18]. In our samples, the activation energy is less than 1.1 eV at a temperature range of 200-

500°C, which means that interstitial oxide ions are responsible for the conductivity. Since there are no changes in cell symmetry observed in these apatites, it is believed that the higher E_a at low temperatures is due to defect trapping at low temperatures [20]. The distance between the lanthanum and the oxygen ion increases as the temperature increases, causing decrease in the electrostatic force which in turn makes the conducting ions flow through the channel more easily. A similar change in activation energy has been observed previously in studies of dense $La_{9.33+x}Si_6O_{26+3x/2}$ [6] and $La_{9.33+x}Si_{6-y}Co_yO_{26+Z}$ [21] pellets.

4   Conclusion

Apatite-type phases $La_{9.33}Si_6O_{26}$ and doped lanthanum silicate apatites have been prepared successfully using a hydrothermal method from La_2O_3, Na_2SiO_4, $BaCO_3$, $CaCO_3$, and $SrCO_3$. The formation of apatite phase during the hydrothermal process took a much shorter time (72 h) than during similar work reported by Ferdov (168 h). The SEM studies show that doping of apatites increases the compactness of the pellet and decreases grain size. However, to get a dense pellet from these apatites, sintering at 1600 °C is needed. The ionic conductivities in these samples are comparable to samples that were prepared by solid state reaction and sol-gel methods.

Acknowledgements

References

[1]   Takeda, N., Itagaki, Y., Aono, H. & Sadaoka, Y., *Preparation and Characterization of Ln_{9.33+x/3}Si_{6−x}Al_xO_{26} (Ln = La, Nd and Sm) with Apatite-Type Structure and Its Application to A Potentiometric O_2 Gas Sensor Potentiometric O_2 Gas Sensor,* Sensor Actuat B-Chem., **115**, p. 455, 2006.

[2]   Sansom, J.E.H., Kendrick, E., Tolchard, J.R., Islam, M.S. & Slater, P.R., *A Comparison of The Effect of Rare Earth vs Si Site Doping on The Conductivities of Apatite-Type Rare Earth Silicates,* J. Solid State Electrochem., **10**, p. 562, 2006.

[3]   Nakayama, S., Sakamoto, M., Highchi, M. & Kodaira, K., *Ionic Conductivities of Apatite Type Nd_X (SiO_4)_6O_{1.5X_i12} (X = 9.20 and 9.33) Single Crystals,* J. Mater. Sci. Lett., **19**, pp. 91-93, 2000.

[4] Nakayama, S., Aono, H. & Sadaoka, Y., *Ionic Conductivity of $Ln_{10}(SiO_4)_6O_3$ (Ln = La, Nd, Sm, Gd and Dy)*, Chem. Lett., **24**, p. 431, 1995.

[5] Kendrick, E., Islam, M.S. & Slater, P.R., *Developing Apatites for Solid Oxide Fuel Cells: Insight Into Structural, Transport and Doping Properties*, J. Mater. Chem., **17**, p. 3104, 2007.

[6] Nakayama, S., Kageyama, T., Aono, H. & Sadaoka, Y., *Ionic Conductivity of Lanthanoid Silicates, $Ln_{10}(SiO_4)_6O_3$ (Ln = La, Nd, Sm, Gd, Dy, Y, Ho, Er and Yb)*, J. Mater. Chem., **5**, pp. 1801-1805, 1995.

[7] Rodríguez, R.E., Fuentes, A.F., Maczka, M., Hanuza, J., Boulahya, K. & Amador, U., *Facile Synthesis, Characterization and Electrical Properties of Apatite-Type Lanthanum Germanates*, Solid State Sci., **8**(2), p. 168, 2006.

[8] Ma, C.Y., Briois, P., Böhlmark, J., Lapostolle, F. & Billard, A., *$La_{9.33}Si_6O_{26}$ Electrolyte Thin Films for IT-SOFC Application Deposited by a HIPIMS/DC Hybrid Magnetron Sputtering Process*, Ionics, 2007.

[9] Vieira, M.M., Oliveira, J.C., Shaula, A.L., Cavaleiro, A. & Trindade, B., *Lanthanum Silicate Thin Films for SOFC Electrolytes Synthesized by Magnetron Sputtering and Subsequent Annealing*, Surf Coat Tech., **206**(14), pp. 3316-3322, 2012.

[10] Gao, W., Liao, H.-L. & Coddet, C., *Plasma Spray Synthesis of $La_{10}(SiO_4)_6O_3$ as a New Electrolyte for Intermediate Temperature Solid Oxide Fuel Cells*, J Power Sources, **179**, 739–744, 2008.

[11]. Dru, S., Meillot, E., Wittmann-Teneze, K. & R. Benoit, M.-L.S., *Plasma Spraying of Lanthanum Silicate Electrolytes for Intermediate Temperature Solid Oxide Fuel Cells (ITSOFCs)*, Surf Coat Tech., **205**(4), pp. 1060-1064, 2010.

[12] Tao, S.W. & Irvine, J.T.S., *Synthesis and Ionic Conduction of Apatite-Type Materials*, Ionics., **6**, pp. 389-396, 2000.

[13] Ioku, K., Yamauchi, S., Fujimori, H., Goto, S. & Yoshimura, M., *Hydrothermal Preparation of Fibrous Apatite and Apatite Sheet*, Solid State Ionics, **151**, pp. 147-150, 2002.

[14] Ferdov, S., Rauwel, P., Lin, Z., Ferreira, R.A.S. & Lopes, A., *A Simple and General Route for The Preparation of Pure and High Crystalline Nanosized Lanthanide Silicates with The Structure of Apatite at Low Temperature*, J Solid State Chem., **183**(11), pp. 2726-2730, 2010.

[15] Riman, R.E., Suchanek, W.L., Byrappa, K., Chen, C.W., Shuk, P. & Oakes, C.S., *Solution Synthesis of Hydroxyapatite Designer Particulates*, Solid state Ionics., **151**, p. 393, 2002.

[16] Bechade, E., Julien, I., Iwata, T., Massona, O., Thomasa, P. & Championa, E., *Synthesis of Lanthanum Silicate Oxyapatite Materials as A Solid Oxide Fuel Cell Electrolyte*, J. Eur. Ceram.Soc., **28**, pp. 2717-2724, 2008.

[17] Savignat, S.B., Vincent, A., Lambert, S. & Gervais, F., *Oxide Ion Conduction in Ba, Ca and Sr Doped Apatite-Type Lanthanum Silicates,* J Mater Chem., **17**, pp. 2078-2087, 2007.

[18] Islam, M.S., Tolchard, J.R. & Slater, P.R., *An Apatite for Fast Oxide Ion Conduction,* Chem. Comm., p. 1486, 2003.

[19] Wenhui, Y., Yaping, G. & Li, L., *Synthesis and Ionic Conduction of Cation-deficient Apatite $La_{9.33-2x/3}M_xSi_6O_{26}$ Doped with Mg, Ca, Sr,* Chin. J. Chem. Eng., **16**(3), pp. 488-491, 2008.

[20] Goodenough, J.B., *Oxide-ion Electrolytes,* Annu. Rev. Mater. Res., **33**, pp. 91-128, 2003.

[21] McFarlane, J., Barth, S., Swaffer, M., Sansom, J.E.H. & Slater, P.R., *Synthesis and Conductivities of the Apatite-type Systems, $La_{9.33+x}Si_{6.y}MyO_{26}$ (M = Co, Fe, Mn) and $La_8Mn_2Si_6O_{26}$,* Ionics., **8**, pp. 149-154, 2002.